Volume 14, No 1 | International Journal of Radiation Research, January 2016

The impact of dose calculation algorithms for peripheral dose distributions of enhanced dynamic and physical wedges

H. Acar[1*], G. Yavas[1], C.Yavas[2]

[1]*Department of Radiation Oncology, Selcuklu Faculty of Medicine, Selcuk University, Turkey*
[2]*Department of Radiation Oncology, Konya Training and Research Hospital, Turkey*

► ***Original article***

Corresponding author:
Dr. Hilal Acar,
Fax: *+ 90 212 446 16 08*
Email:*hilalacar@hotmail.com*

Revised: March 2015
Accepted: April 2015

Int. J. Radiat. Res., January 2016; 14(1): 17-24

DOI: 10.18869/acadpub.ijrr.14.1.17

ABSTRACT

Background: In radiation therapy, the peripheral dose is important when anatomical structures with very low dose tolerances are involved. In this study, the two available calculation algorithms of the Varian Eclipse 8.6 treatment planning system(TPS), the anisotropic analytic algorithm (AAA) and pencil-beam convolution (PBC) was used to compare measured and calculated peripheral dose distribution of physical wedged (PW) and enhanced dynamic wedged fields (EDW). ***Materials and Methods***: Peripheral dose measurements were carried out for 6 and 18 MV photons using a 0.6cc Farmer-type ionization chamber in the slab phantom. Measurements were performed using 15°, 30°, 45° and 60° PW and EDW for three different field sizes at d_{max} and up to a maximum distance of 50 cm beyond the field edges. peripheral dose was further computed using two different algorithms of a TPS. The measured and calculated datas were then compared to find which algorithm calculates peripheral dose distribution more accurately. ***Results:*** Both algorithms from the TPS adequately model the peripheral dose distribution up to 45 degrees. For large field sizes with 60^0 EDW, the largest deviation between calculated and measured dose distribution is less than 3.5% using the AAA, but can increase up to 9.7% of the distribution using PBC. ***Conclusion:*** The AAA models wedged peripheral dose distributions more accurately than the PBC does for all studied conditions; the difference between the algorithms are more significant for large wedge angles and large field sizes. It must be emphasized that the use of PBC for planning large-field treatments with 60^0 EDW could lead to inaccuracies of clinical significance.

Keywords: *Physical wedge, enhanced dynamic wedge, peripheral dose distribution, calculation algorithms, AAA, PBC .*

INTRODUCTION

The peripheral dose is the radiation dose received at points beyond the collimated radiotherapy field edge. So as to ensure that radiosensitive tissues outside of the beam do not receive doses approaching their tolerance levels, detailed knowledge of magnitude and spatial distribution of the peripheral dose may be necessary [(1)].

The peripheral radiation dose can be important clinically, potentially affecting cataract formation, gonadal function and fertility. The peripheral dose can also be responsible for exposure to the fetus in a pregnant woman, and dose to breast and other tissues for which radiation induced carcinogenesis may be concern [(2)].

The Varian Eclipse (Varian Medical Systems, Palo Alto, CA) version 8.6 treatment planning system (TPS) supports two different dose

[DOI: 10.18869/acadpub.ijrr.14.1.17]

calculation methods: one based on the superposition of energy deposition kernels of pencil beams (PBC)[3], and one uses pre-calculated Monte Carlo simulations based on a convolution model Analytical Anisotropic Algorithm (AAA) [4,5]. PBC algorithm uses experimental measurements as part of the beam configuration [6]. In contrast, AAA, the pencil beams are compiled from previous Monte Carlo (MC) calculations and then adjusted to fit measurements [7–11]. Thus, in both cases, accurate dose calculation is dependent on the introduction of accurate measured data in the system.

However, TPSs are not commissioned for out-of-field dose calculations [12, 13] and the accuracy of TPS dose calculations is known to decrease beyond the borders of the treatment fields. Also, the true accuracy of specific TPSs for out-of-field dose is not well documented in the literatüre [14]. As far as we know there is no study that examine of accuracy of the treatment planning system algorithms for the wedged peripheral dose distribution.

The main purpose of this paper was to investigate the accuracy of dose calculation algorithms of Eclipse TPS for out of field doses. The peripheral dose distribution of physical wedge (PW) and Enhanced Dynamic Wedge (EDW) were measured using 0.6 cc farmer type ionization chamber. The measured datas were then compared with those calculated by the TPS using the PBC and the AAA.

MATERIALS AND METHODS

Ionization chamber measurements

Varian Clinac-DHX (Varian Medical Systems, Palo Alto, CA) linear accelerator which is equipped with two different types of wedges was used in this study. Peripheral dose measurements were performed using a 0.6 cm^3 Farmer-type ionization chamber (PTW 30010, PTW, Friedberg, Germany) inserted into a 40 × 15 × 120 cm^3 (width × height × length) water-equivalent plastic phantom (RW3 Slab phantom, PTW, Friedberg, Germany). Great care was taken to ensure that there was no air gap while aligning the slabs. The chamber was connected to a calibrated electrometer (PTW Unidos Webline, Friedberg, Germany). For all measurements, the ionization chamber was placed at a depth of dose maximum in the phantom (midplane) at 100 cm source to surface distance (SSD) for 6 MV and 18 MV photons. In general, published data [15,16] show that the depth dependence of peripheral dose distribution is small. Therefore, measurements were made only at the dose maximum depth (1.5 cm for 6 MV and 3.5 cm for 18 MV). All measurements were done using farmer type ionization chamber to avoid systematic errors due to different measurement techniques.

In this study 15°, 30°, 45° and 60° physical and enhanced dynamic wedges were used. The 15° and 30° PW were made of Fe (cold-rolled steel) with nominal density of 7.8 g/cm^3 whilst 45° and 60° were made of Pb (lead-calcium-tin alloy) with nominal density of 11.3 g/cm^3. Varian EDW (Varian Medical Systems, Palo Alto, CA) consists in the simulation of a PW by moving one of the Y collimator jaws during the irradiation with variable speed from its maximum open position to 0.5 cm of the opposite jaw and adjusting dose rate during treatment.

The field size was maintained as 5 × 5 cm^2, 10 × 10 cm^2 and 15 × 15 cm^2. The peripheral doses were measured from 0.5 cm up to 50 cm distances from the geometric field edge in increments of 0.5 cm at the heel side of the wedge field. The collimator angle was 0^0. Each measurement was repeated three times and the mean value of the readings were noted. The standard error was found to be within 1%. All the datas were normalized to central axis at depth of dose maximum. The linear accelerator output was checked and monitored on a daily basis before each set of measurements.

As pointed out in the TG – 36 [17] report, the contribution of neutrons to the total peripheral dose is small near the beam edge. The National Council of Radiation Protection [18] considers the risk of long-term biological effects of incidental from the linear accelerator to be negligible. Because of this reason, these measurements did not account for dose contributions from photoneutrons.

[DOI: 10.18869/acadpub.ijrr.14.1.17]

External beam treatment planning calculations

The TPS calculation algorithm accuracy was evaluated by comparing measurements and calculations performed under the same conditions, based on a phantom imaged by CT.

The 40×15×120cm^3 water-equivalent plastic phantom was imaged by a computerized tomography (Toshiba Aquilion; Toshiba Medical Systems, Japan) to obtain three dimensional (3D) image data sets of 3 mm slices and transferred to the 3D TPS.

The PW and EDW beams were created with the collimator and gantry orientation as in solid water phantom and appropriate field size, wedge angle, weight point definition, normalization, etc, imitating the measurements under real conditions in solid water phantom. All plans were initially calculated with a PBC algorithm. Plans were then recomputed (keeping everything same) within Eclipse using AAA. All calculations were performed on 2 mm dose grid.

The AAA is one of the models that incorporate electron transport for dose calculation. It is a three-dimensional PBC/superposition algorithm that uses Monte Carlo-derived scatter kernels tomodel primary photons (primary source), scattered extra focal photons and electrons scattered from the beam limiting devices (electron contamination source). The primary source is the point source located at the target plane. It models the bremsstrahlung photons created in the target that do not interact in the treatment head. The extra-focal source is a Gaussian plane source located at the bottom plane of the flattening filter. It models the photons that result from interactions in the accelerator head outside the target, primarily in the flattening filter, primary collimators and secondary jaws. Electron contamination is modeled with a depth-dependent curve that describes the total amount of electron contamination at a certain depth. The final dose distribution is computed by the superposition of the dose calculated by the photons and electron convolutions. The kernels are calculated using a sum of six depth-dependent weighted exponentials, defining the lateral scattering in order to fit the Monte Carlo-derived pencil beam scatter [19]. A more detailed description of the algorithm can be found in the study made by Tillikainen L *et al.* [20].

The resulting calculated plans were analyzed taking into consideration the point doses on dose maximum depth. The peripheral doses were recorded from the TPS using two different algorithms and compared with the measured values.

RESULTS AND DISCUSSION

Figures 1a-c show the measured percentage peripheral dose distribution for different wedge filters between 0.5 cm to 50 cm distance from the field edge at the heel side of the wedge field at 1.5 cm depth of 6 MV photons for 5×5 cm^2, 10×10 cm^2 and 15×15 cm^2 fields respectively. For 18 MV, the same data were shown in figures 2 a-c. Three conclusion can be easily drawn from these figures. First, peripheral dose increases with the increase in field size. This means that peripheral dose is dependent on field size. The variation with field size is significant only for small fields. The percentage difference between 5×5 cm^2 and 10×10 cm^2 is much larger than the difference between 10×10 cm^2 and 15×15 cm^2 fields. Secondly, peripheral dose is dependent on energy. As energy increases peripheral dose decreases. Finally, the peripheral dose is less for the EDW when compared to the physical wedges. One of the reason for that lies in scatter outside the hard wedged field, due to the interaction of the beam with the material of the mechanical wedge. Clinically, this is an advantage of EDW wedged field. Another reason could be that EDW is placed at a considerable distance from patient and it does not have varying physical thickness as that of the physical wedge. The differential thickness across the physical wedge would result in more scattered radiation being produced.

EDW fields in general use less monitor units than PW fields, although beam-on time may be larger for large wedge angles with large field sizes due to a variable dose rate being used for EDW fields. It would be expected that physical

[DOI: 10.18869/acadpub.ijrr.14.1.17]

wedged peripheral dose distributions would be approximately two times larger than EDW peripheral dose distributions due to an increase in leakage radiation which is related to increased MUs. Furthermore, it is expected that these differences would be observed at longer distances from the field edge, where the leakage radiation dominates [21-23]. Data presented here supports this expectation. Physical wedged peripheral dose distributions are comparable to EDW peripheral dose distributions at distances less than 10 cm from the field edge and become almost two times greater at longer distances. This is due to approximately equivalent internal scatter contribution for EDW and PW fields. Also, the wedge provides additional shielding for collimator scatter and leakage radiation in comparison to EDW fields. The effect of this shielding is largest underneath the wedge and close to the field edge and eventually becomes smaller at distances far from the field edge.

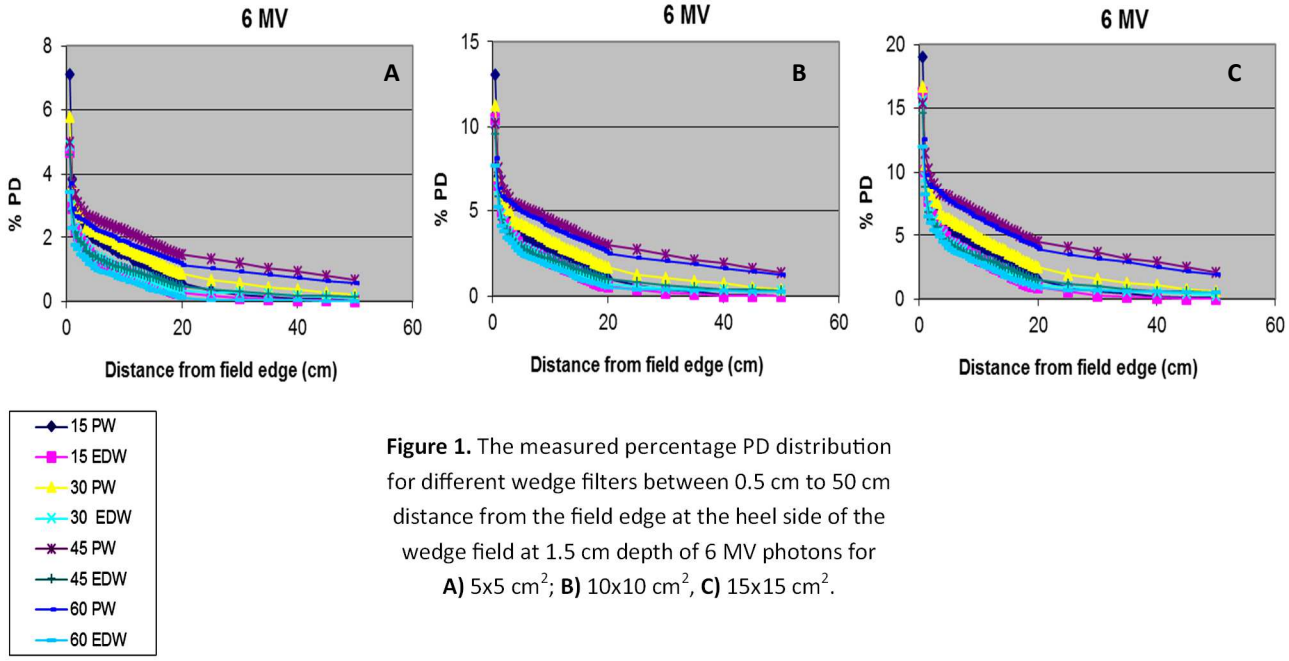

Figure 1. The measured percentage PD distribution for different wedge filters between 0.5 cm to 50 cm distance from the field edge at the heel side of the wedge field at 1.5 cm depth of 6 MV photons for **A)** 5x5 cm^2; **B)** 10x10 cm^2, **C)** 15x15 cm^2.

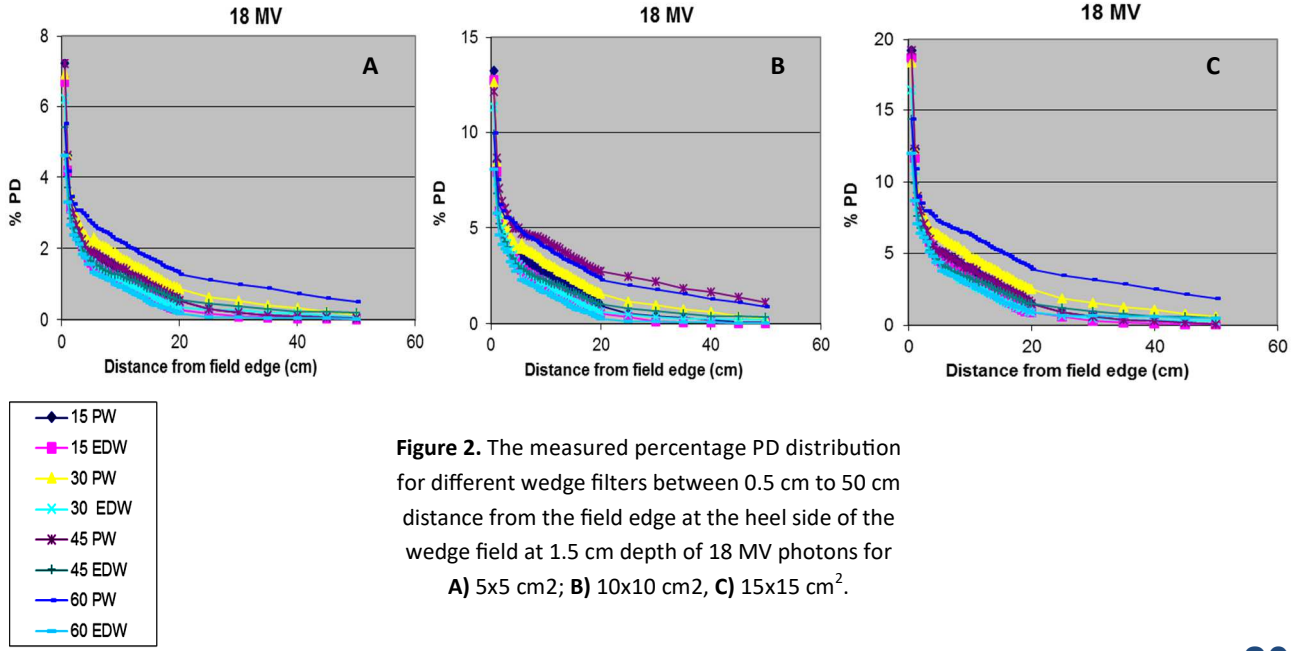

Figure 2. The measured percentage PD distribution for different wedge filters between 0.5 cm to 50 cm distance from the field edge at the heel side of the wedge field at 1.5 cm depth of 18 MV photons for **A)** 5x5 cm2; **B)** 10x10 cm2, **C)** 15x15 cm^2.

[DOI: 10.18869/acadpub.ijrr.14.1.17]

This is important information when choosing wedge filters for treatment of patients with radiosensitive structures such as eye lens, thyroid gland, gonads, fetus, etc. which need to be protected. The data presented here demonstrates that the use of EDW with a small wedge angle is a good choice for the treatment of these patients. The dose to critical structures located near the field edge may be comparable to open field doses. However, the whole body dose will be higher for EDW fields.

The measured and TPS calculated percentage peripheral dose at a depth of 1.5 cm for 6 MV photon beam is shown for 15^0 wedge angle with 5×5 cm^2 field in figure 3(a). The percentage peripheral dose of 45^0 wedge angle with 10×10 cm^2 field size and that of 60^0 wedge angle with 15×15 cm^2 field size are shown in figure 3(b) and figure 3(c) respectively.

The measured and TPS calculated percentage peripheral dose at a depth of 3.5 cm for 18 MV photon beam is shown for 15^0 wedge angle with 5×5 cm^2 field in figure 4(a). The percentage peripheral dose of 45^0 wedge angle with 10×10 cm^2 field size and that of 60^0 wedge angle with 15×15 cm^2 field size are shown in figure 4(b) and 4(c) respectively.

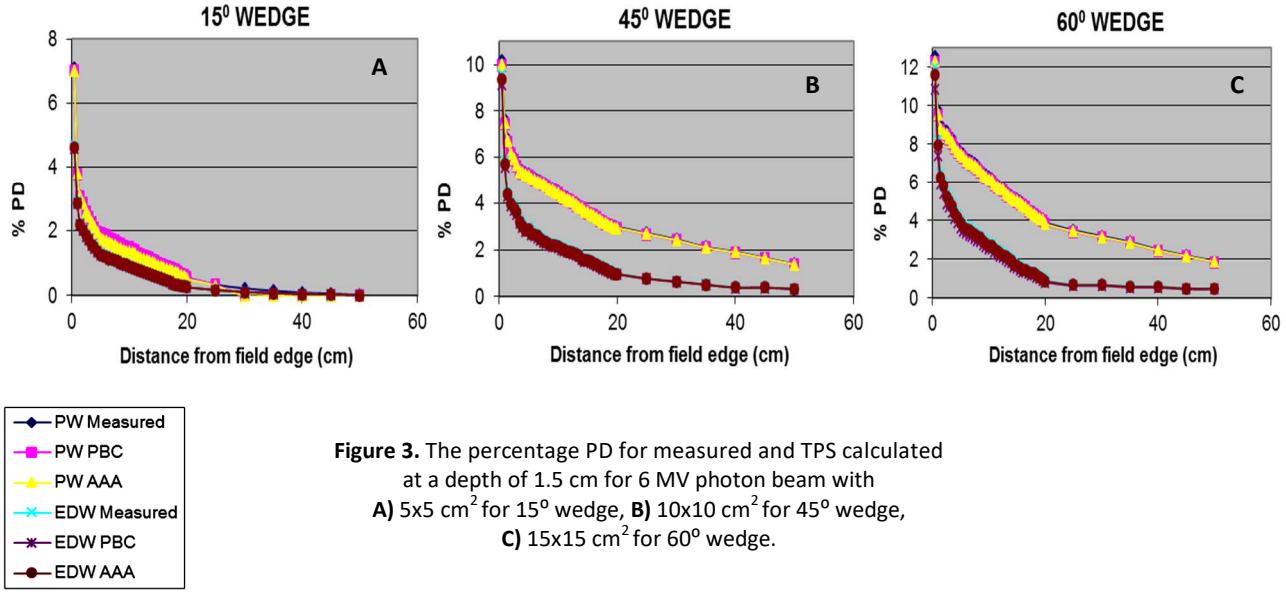

Figure 3. The percentage PD for measured and TPS calculated at a depth of 1.5 cm for 6 MV photon beam with **A)** 5x5 cm^2 for 15^o wedge, **B)** 10x10 cm^2 for 45^o wedge, **C)** 15x15 cm^2 for 60^o wedge.

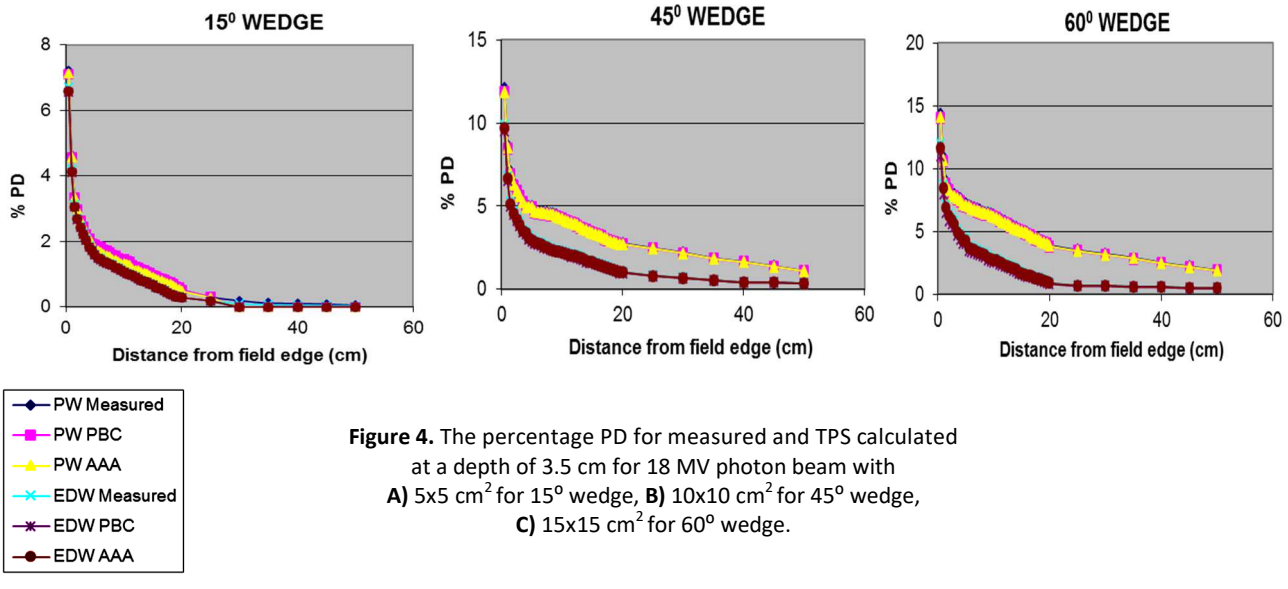

Figure 4. The percentage PD for measured and TPS calculated at a depth of 3.5 cm for 18 MV photon beam with **A)** 5x5 cm^2 for 15^o wedge, **B)** 10x10 cm^2 for 45^o wedge, **C)** 15x15 cm^2 for 60^o wedge.

[DOI: 10.18869/acadpub.ijrr.14.1.17]

It is seen from the figures 3 and 4 that the most important difference between the two algorithms can be observed at 0.5 cm distance from the field edge as the distance from the field edge increase the difference decreases. The difference between the calculation algorithms increases for larger wedge angles and larger field sizes. There is slight decrease in difference between calculation algorithms and measurements with increasing beam energy. The TPS calculated peripheral dose underestimate the measured ones.

It is concluded from the figures 3 (a) - (c) that for physical wedges and 6 MV photon energy, max 2.8 % difference is observed between measurement and PBC calculated percentage peripheral dose for 60 degree wedge with 15×15 cm^2 field. The difference is 1.9 % for the same field size and wedge angle if AAA algorithm is used. The difference between the measured and calculated peripheral dose decreases with decreasing field size and wedge angles. The minium difference is 1.2 % for PBC algorithm when 15 degree wedge and 5×5 cm^2 field size is used. There is no significant change in difference between measurements and calculation algorithms for 18 MV as it can be seen from figure 4 (a) - (c).

It is seen from the figures 3 (a) - (c) that for enhanced dynamic wedges and 6 MV photon energy maximum 9.7 % and 3.5 % differences are found for 60^0 wedge with 15×15 cm^2 field between measurement and calculation algorithms PBC and AAA calculated percentage peripheral dose respectively. The difference between the measured and calculated peripheral dose decreases with decreasing field size and wedge angles. The minimum difference is 2.5 % for PBC algorithm and 2 % for AAA algorithm when 15^0 wedge and 5×5 cm^2 field size was used.

For 18 MV, there is a slight decrease in difference between measured and calculated peripheral dose as it can be seen from figure 4 (a) - (c). The maximum differences are 8.5 % and 3.1 % for PBC and AAA algorithms respectively for 60^0 wedge with 15×15 cm^2 field. The minimum 2.2 % and 1.8 % are differences are seen for 15^0 wedge and 5×5 cm^2 field size for PBC and AAA algorithms respectively.

The variation can be explained by taking into account the fact that the PBC calculates the wedged distribution using a superposition of many rectangular fields without considering extrafocal radiation[24]. The fact that many open fields are superposed to model the EDW, considering that inaccuracies are a consequence of the open field modeling, yields greater inaccuracies for this kind of treatment. On the other hand, the AAA calculates the open-field distribution considering primary and extrafocal radiation from head-scatter effects[25,26]. Therefore, because the open-field modeling is better with the AAA, wedged dose distributions calculated with this algorithm (by the same method as the PBC) are closer to measured ones.

Howel and et al[14] investigates the accuracy of out of field dose calculation by Eclipse and resulted that The Eclipse AAA models extra-focal photon radiation (all photons emerging from outside the target) using a finite-size virtual source (referred to as the second source). The second source has a Gaussian intensity distribution. According to the Eclipse manual[27] the second source energy fluence is defined at an arbitrary plane and is computed by adding the contributions from each element of the source for each pixel in the destination fluence array. The contribution is scaled by the Gaussian weight of the source element, by the inverse square of the distance between the elements at the source and destination planes, and by the cosine of the ray angle. They concluded that in contrast to how the out-of-field dose is modeled in Eclipse, the out-of-field dose is actually composed of scatter and leakage radiation and is underestimated by the Gaussian intensity distribution. The finding of this study supports their results.

In all cases, it is easy to note that the AAA models the dose distribution more accurately than the PBC does. Both algorithms from the TPS adequately model the peripheral dose distribution up to 45 degrees. For large field sizes with 60 degrees EDW, the largest deviation between calculated and measured dose distribution is less than 3.5 % using the AAA, but can increase up to 9.7 % of the distribution using PBC.

[DOI: 10.18869/acadpub.ijrr.14.1.17]

CONCLUSION

In the present study, the unwanted radiation has been measured as a function of the distance outside the primary beam, field size and beam energy. Complete knowledge of the peripheral doses is cruical in proper choice of particular wedge system in clinical use.

The study concluded that for all investigated conditions, the AAA models wedged dose distributions more accurately than the PBC does; the difference between the algorithms are more significant for large wedge angles and large field sizes. It must be emphasized that the use of PBC for planning large-field treatments with 60^0 EDW could lead to inaccuracies of clinical significance.

Conflicts of interest: *none to declare.*

REFERENCES

1. McParland BJ and Fair HI (1992) A method of calculating peripheral dose distributions of photon beams below 10 MV. *Med Phys,* ***19(2):*** *283-293.*
2. Antypas C, Sandilos P, Kouvaris J, Balafouta E, Karinou E, Kollaros N, Vlahos L (1998) Fetal dose evaluation during breast cancer radiotherapy. *Int J Radiation Oncology Biol Phys,* ***40(4):*** *995-999.*
3. Storchi P and Woudstra E (1996) Calculation of the absorbed dose distribution due to irregularly shaped photon beams using pencil beam kernels derived from basic beam data. *Phys Med Biol,* ***41 (4):*** *637–656.*
4. Fogliata A, Nicolini G, Vanetti E, Clivio A, Cozzi L (2006) Dosimetric evaluation of anisotropic analytical algorithm for photon dose calculation: fundamental characterization in water. *Phys Med Biol,* ***51(6):****1421–1438.*
5. Aspradakis MM, Morrison RH, Richmond ND, Steele A (2003) Experimental verification of convolution/ superposition photon dose calculations for radiotherapy treatment planning. Phys Med Biol, **48:**2873–93.
6. Storchi PMR, van Battum LJ, Woudstra E (1999) Calculation of a pencil beam kernel from measured photon beam data. *Phys Med Biol,* ***44:****2917–28.*
7. Van Esch A, Tillikainen L, Pyykkonen J, Tenhunen M, Helminen H, Siljamaki S, Alakuijala J, Paiusco M, Iori M, Huyskens DP (2006) Testing of the analytical anisotropic algorithm for photon dose calculation. Med Phys, **33:**4130 –48.
8. Bragg CM and Conway J (2006) Dosimetric verification of the anisotropic analytical algorithm for radiotherapy treatment planning. *Radiother Oncol,* ***81:*** *315–23.*
9. Van Esch A, Tillikainen L, Pyykkonen J, Tenhunen M, Helminen H, Siljamaki S, *et al.* (2006)Testing of the analytical anisotropic algorithm for photon dose calculation. *Med Phys,* ***33:****4130–47.*
10. Knoos T, Wieslander E, Cozzi L, Brink C, Fogliata A, Albers D, *et al.* (2006) Comparison of dose calculation algorithms for treatment planning in external photon beam therapy for clinical situations. *Phys Med Biol,* ***51:****5785–807.*
11. Fogliata A, Nicolini G, Vanetti E, Clivio A, Cozzi L (2006) Dosimetric validation of the anisotropic analytical algorithm for photon dose calculation: fundamental characterization in water. *Phys Med Biol,* ***51:****1421–38.*
12. Aspradakis MM, Morrison RH, Richmond ND, Steele A (2003) Experimental verification of convolution/ superposition photon dose calculations for radiotherapy treatment planning. *Phys Med Biol,* ***48:****2873–93.*
13. Das IJ, Cheng CW, Watts RJ, Ahnesjo A, Gibbons J, Li XA, Lowenstein J, Mitra RK, Simon WE, Zhu TC (2008) Accelerator beam data commissioning equipment and procedures: report of the TG-106 of the therapy physics committee of the AAPM. *Med Phys,* ***35:*** *4186–215.*
14. Rebecca M, Howell, Sarah B Scarboro, S F Kry, and Derek Z Yaldo (2010) Accuracy of out-of-field dose calculations by a commercial treatment planning system. *Phys Med Biol,* ***55 (23):*** *6999–7008.*
15. Van der Giessen (1994) PH Calculation and measurement of the dose at points outside the primary beam for photon energies of 6, 10 and 23 MV. *Int J Radiat Oncol Biol Phys,* ***30:*** *1239-46.*
16. Mutic S, Esthappan J, Klein EE (2002) Peripheral dose distributions for a linear accelerator equipped with a secondary multileaf collimator and universal wedge. *J Appl Clin Med Phys,* ***3:*** *302-9.*
17. Stovall M, Blackwell CR, Cundiff J, Novack D, Palta JR, Wagner LK (1995) Fetal dose from radiotherapy with photon beams: Report of AAPM Radiation Therapy Committee Task Group No. 36. *Med Phys,* ***22:*** *62-82.*
18. National Council on Radiation Protection (1980) Influence of dose and its distribution in time on dose -response relationship for low-LET radiations. *Report No. 64. Bethasda, MD.*
19. Kan MWK, Cheung JYC , Leung LHT, Lau BMF, Yu PKN (2011) The accuracy of dose calculations by anisotropic analytical algorithms for stereotactic radiotherapy in nasopharyngeal carcinoma. *Phys Med Biol,* ***56:*** *397–413*
20. Tillikainen L, Helminen H, Torsti T, Siljamaki S, Alakuijala J, Pyyry J, Ulmer W (2008) A 3D pencil-beam-based superposition algorithm for photon dose calculation in heterogeneous media. *Phys Med Biol,* ***53:*** *3821–39.*
21. Francois P, Beurtheret C and Dutreix A (1988) Calculation of the dose delivered to organs outside the radiation beams. *Med Phy,* ***15(6):*** *879-883.*
22. Van der Gissen PH and Hurkmans CW (19930 Calculation and measurement of the dose to points outside the primary beam for ^{60}Co gamma radiation. *Int J Radiat Oncol Biol Phys,* ***27:*** *717-724.*
23. Greene D, F.Inst. Gou-Long Chu, DW Thomas M (1985) Dose levels outside radiotherapy beams. *Br J Radiol,* ***58:*** *543.*

[DOI: 10.18869/acadpub.ijrr.14.1.17]

24. Storchi P and Woudstra E (1996) Calculation of the absorbed dose distribution due to irregularly shaped photon beams using pencil beam kernels derived from basic beam data. *Phys Med Biol,* ***41(4):*** *637–656.*
25. Sievinen J, Ulmer W, Kaissl W (2005) AAA photon dose calculation model in Eclipse. Palo Alto (CA): Varian Medical Systems. [RAD #7170B]
26. Varian Medical Systems (2005) The reference guide for Eclipse algorithms. Palo Alto (CA): Varian Medical Systems. [P/N B401653R01M]
27. Varian Medical Systems I. (2008) Eclipse Algorithms Reference Guide, Version 86. Palo Alto, CA: Varian Medical Systems.

[DOI: 10.18869/acadpub.ijrr.14.1.17]